J. Int. Sci. Technol. 2020, 8(2), 41-50 Article

Journal of Integrated
SCIENCE & TECHNOLOGY

Electrochemistry of Ferrocene in different Room Temperature Ionic Liquids with Platinum and Gold Electrodes

Virendra V. Singh, Lokesh K. Pandey, Pushpendra K. Sharma, Utpal Biswas, Kumaran Ganesan, Mannan Boopathi*

Defence Research and Development Establishment, Jhansi Road, Gwalior-474002, Madhya Pradesh, India

Received on: 16-Oct-2020, Accepted and Published on: 24-Nov-2020

ABSTRACT

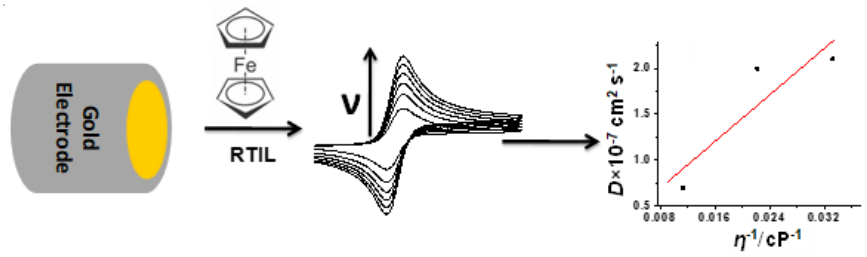

Electrochemical characterization of ferrocene (Fc) was investigated to find out diffusion coefficient (D), heterogeneous rate constant (kº), and relationship between D and kº with Pt and Au electrode in three common room temperature ionic liquids (RTILs) containing namely 1-butyl-1-methyhlpyrrolidinium bis (trifluoromethylsulfonyl) imide, 1-ethyl-3-methylimidazolium trifluoromethylsulfonate and triethylsulfonium bis (trifluoromethylsulfonyl) imide by utilizing cyclic voltammetry and impedance spectroscopy. The D, double layer capacitance (Cdl) and apparent activation energy (ΔGexp) of Fc was deduced in order to elucidate the role of RTIL on the electrode kinetics. The kº of Fc was estimated by electrochemical impedance spectroscopy by using the Randles equivalent circuit as the model. A graph between ln (kº) versus ln (η) suggests that Fc redox process in RTIL with Pt and Au electrodes are adiabatic. The calculated diffusion coefficients and rate constant were of the order of 10−7 cm2 s−1 and 10−2 cm s−1, respectively.

Keywords: Room temperature ionic liquids, heterogeneous rate constant, Ferrocene, diffusion coefficient, kinetic parameters

INTRODUCTION

Room Temperature Ionic Liquids (RTILs) has attracted greater interest in recent years as it exemplify its versatile uses as electrolyte in many industrial applications as a potential reaction media.[1-4] RTILs are distinct classes of solvents comprising of numerous combination of different cations and anions posses unique physiochemical properties such as non-volatility, high thermal and chemical stability; large conductivity, wide electrochemical window and high flexibility are of increasing interest to various electrochemical applications.[1-4] As a consequence of their peculiar properties RTILs are often regarded as promising designer solvents or as an alternative to organic solvents and have used extensively as electrolyte for various applications such as organic synthesis[1], solar cell,[5-6] electrochemical sensors[2] and electrodeposition of various metals.[3] Air and moisture stable RTILs[4] have attracted much attention as an alternative solvent media for electrochemistry and act as intermediate between that of aqueous and molecular organic solvents.[1-4] Owing to higher cathodic and anodic limit of RTIL, it shows higher electrochemical potential windows that largely non accessible in aqueous electrolytes allowing the electrodeposition of metals and semiconductors. Intrinsic conductivity of RTILs avoid the use of supporting electrolyte and make it suited to improve the energy storage that are otherwise out of the potential range of traditional solvents.[5-10]

To date, voltammetric measurements in RTILs have mainly employed quasi-reference electrodes, mostly Pt or Ag wire electrode. To overcome this problem, many authors use a quasi-reference electrode in combination with an electrochemically

*Corresponding Author: Dr. Mannan Boopathi
Tel: +919685918269
Email: boopathi@drde.drdo.in

Cite as: *J. Int. Sci. Technol., 2020, 8(2), 41-50.*

 ISSN: 2321-4635 http://pubs.iscience.in/jist

reversible ferrocene/ferrocenium (Fc/Fc^+) or cobaltaocenium/cobaltacene (Cc^+/Cc) redox couple as it exhibits nearly ideal reversibility in most of the organic solvent and it is also recommended as potential referencing by IUPAC, also both systems are considered as likely "ideal" potential standards.[11-12] Moreover, heterogeneous rate constant (k^o), diffusion coefficient (D) and double layer capacitance (C_{dl}) of Fc in RTILs are of significant interest in both fundamental and applied electrochemistry as it provides the rate of charge transfer reactions.[13-17] Owing to higher viscosity of RTIL, k^o of Fc was expected to lower when compared to organic solvents.[18-20]

In the present work, electrochemical characterization of Fc was conducted with Pt and Au electrode in three different ionic liquid namely 1-butyl-1-methyhlpyrrolidinium bis (trifluoromethylsulfonyl) imide [(C_4mpyrr) (NTf_2)], 1-ethyl-3-methylimidazolium trifluoromethylsulfonate [(C_2mim) (OTf)] and triethylsulfonium bis (trifluoromethylsulfonyl) imide [(C_2sulf) (NTf_2)] as these ionic liquids are used as a very versatile electrolyte in many applications including electrochemical energy storage, sensor and super capacitor.[18-20] Hence, the acquisition of accurate and reliable values of working potential, D, k^o and C_{dl} are of significant important in these electrochemical systems. The heterogeneous rate constant of Fc is estimated by the EIS and further it is correlated with the viscosity of RTIL.

Experimental Section

2.1. Chemicals and reagents. RTILs 1-butyl-1-methyhlpyrrolidinium bis (trifluoromethylsulfonyl) imide [(C_4mpyrr) (NTf_2)], 1-ethyl-3-methylimidazolium trifluoromethylsulfonate [(C_2mim) (OTf)], triethylsulfonium bis (trifluoromethylsulfonyl) imide [(C_2sulf) (NTf_2)] and ferrocene (Fc) [Fe (C_2H_5)$_2$, 98%] were received from Sigma-Aldrich and used as received.

2.2. Instruments and electrochemical studies: Electrochemical experiments were performed at room temperature 25 ± 2 °C by using potentiostat/galvanostat with a frequency response analyzer (Autolab-302 with FRA-II, The Netherlands).

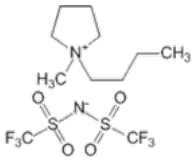

1-butyl-1-methylpyrrolidinium bis(trifluoromethylsulfonyl)imide

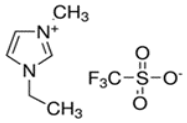

1-ethyl-3-methylimidazolium trifluoromethyl sulfonate

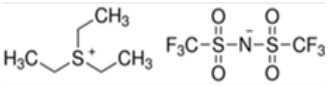

Triethylsulfonium bis(trifluoromethylsulfonyl)imide

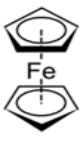

Ferrocene

Figure 1: Structure of RTIL and Ferrocene

The electrochemical experiments are performed in a three electrode cell system comprising of a Pt or Au working, platinum wire quasi-reference and platinum counter electrodes, respectively of Metrohm make. Cyclic voltamogram and impedance spectra are recorded at room temperature by purging the nitrogen for 10 min prior to measurements in order to remove dissolved oxygen. Experiments are performed utilizing the iR compensation method. Figure 1 depicts the structure of RTILs and Fc used in this study.

Result and Discussion

3.1. Electrochemical behavior of Fc in different RTIL with Pt electrode

The electrochemical redox property of Fc was studied in three different RTILs with Pt electrode and the resultant CVs are included as Figure2 after iR drop correction. The characterization of Fc in these RTILs was chosen due to their higher electrochemical potential window, thermal stability and higher stability towards moisture.[21]

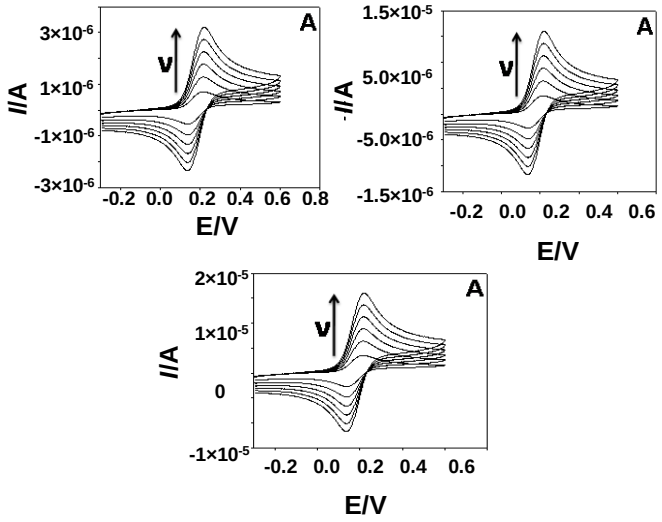

Figure 2. CVs for the oxidation of 0.01 M Fc with Pt electrode in the RTILs: (A) [(C_4mpyrr) (NTf_2)], (B) [(C_2mim) (OTf)] and (C) [(C_2sulf) (NTf_2)] at scan rates of 25, 50, 75, 100, 125 and 150 mV/s.

For the understanding of redox characteristic of Fc/Fc^+ couple, CVs for the oxidation of 0.01 M Fc with Pt electrode were recorded between -0.3 V and + 0.6 V at different scan rate from 25 to 150 mV s^{-1} with a step potential of 25 mV s^{-1} and depicted in Fig 1(A) [(C_4mpyrr) (NTf_2)], (B) [(C_2mim) (OTf)] and (C) [(C_2sulf) (NTf_2)] against a Pt quasi-reference electrode. The recorded CVs are stable with no potential shift observed between the first and final CV approaching reproducibility less than ± 1mV for experiments conducted over a period of three days. It can be clearly seen from Figure 2 that the Fc is oxidized to Fc^+ ion at the peak potential of (A) +0.210 V in [(C_4mpyrr) (NTf_2)], (B) +0.0809 V in [(C_2mim) (OTf)] and (C) +0.273 V in [(C_2sulf) (NTf_2)] vs. Pt (at 50 mV s^{-1}) and reduced back to Fc at the potential of +0.130 V, +0.010 V and +0.180 V in [(C_4mpyrr) (NTf_2)], [(C_2mim) (OTf)] and [(C_2sulf) (NTf_2)], respectively (at 50 mV s^{-1}), showing one electron involvement for the redox system Fc/ Fc^+ couple in RTIL.[22] Based on the above observation, the following mechanism is proposed for the oxidation of Fc to Fc^+ with Pt electrode:

$$[RTIL] + Fc \leftrightarrow Fc^+[RTIL] + 1e^-$$

The value of peak separation (ΔE_p), half wave potential ($E_{1/2}$), and I_{pa}/I_{pc} of the Fc, in different RTILs are investigated in this study and summarized in Table 1.The ΔE_p of Fc with Pt electrode in RTIL [(C_4mpyrr) (NTf_2)] and [(C_2mim) (OTf)] at varying sweep rate is constant which shows the reversible behavior of ferrocene. Nevertheless, in case of [(C_2sulf) (NTf_2)], peak potential separation increased with sweep rate, indicates quasi-reversible redox behavior of Fc with Pt electrode.[3, 23-25.]

3.2. Effect of scan rate on Ferrocene at Pt electrode

Scan rate variation studies were carried out in order to know the nature of redox behavior of Fc with Pt electrode in all three RTILs by varying scan rate from 25 mV/s to 150 mV/s with an increment of 25 mV/s. The resultant CVs are shown in Figure 2, an increase in peak current was observed with increase in scan rate in the forward and reverse scans in different RTILs.

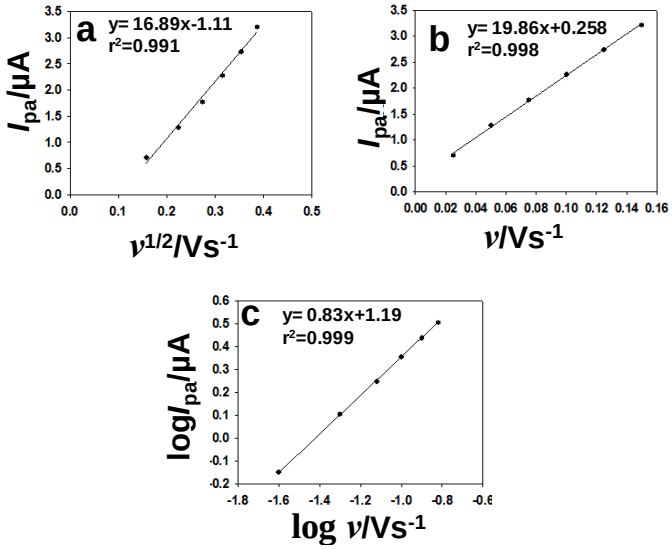

Figure 3. Various graphs obtained from the oxidation of 0.01 M Fc in [C_4mpyrr) (NTf_2)] with Pt electrode: (a) Peak current (I_{pa}) vs. root square scan rate ($v^{1/2}$), (b) Peak current (I_{pa}) vs. scan rate (v) and (c) log I_{pa} vs. log v (scan rate).

Figures 3, 4, and 5 show the various data analysis graphs obtained from the study of CV for Fc with Pt electrode in [(C_4mpyrr) (NTf_2)], [(C_2mim) (OTf)] and [(C_2sulf) (NTf_2)], respectively. Fig 3a shows a plot of peak current (I_{pa}) vs. root scan rate ($v^{½}$) for Fc in [(C_4mpyrr) (NTf_2)], moreover, Figure 4a, and Figure 5a shows the same plot for Fc in [(C_2mim) OTf)] and [(C_2sulf) (NTf_2)], respectively. In all cases a high degree of linearity with anodic peak is observed for Fc with Pt electrode (least square correlation coefficient 0.991 in [(C_4mpyrr) (NTf_2)], 0.975 in [(C_2mim) (OTf)] and 0.974 in [(C_2sulf) (NTf_2)]). These results shows the electrochemical oxidation process of Fc in all RTILs is diffusion controlled.[3] It has been observed that regression lines in figure do not pass through the origin as reported earlier in case of RTILs.[3,24]

Moreover, the anodic current (I_{pa}) vs. scan rate (v) variation profiles were also plotted (Figure 3b, 4b, and 5b) and it also shows good linearity with least square correlation coefficient 0.998 in [(C_4mpyrr) (NTf_2)], 0.989 in [(C_2mim) (OTf)] and 0.919 in [(C_2sulf) (NTf_2)]). Therefore, to further confirm the behavior of Fc

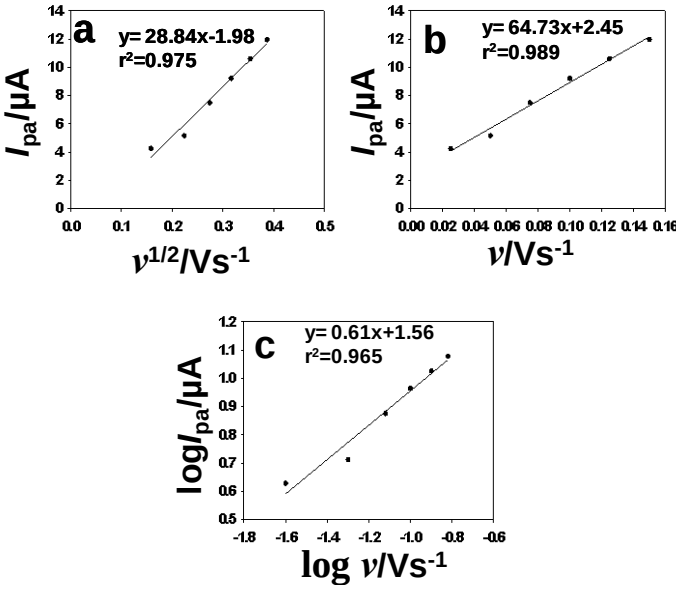

Figure 4. Various graphs obtained from the oxidation of 0.01 M Fc in [(C_2min) (OTf)] with Pt electrode: (a) Peak current (I_{pa}) vs. root square scan rate ($v^{1/2}$), (b) Peak current (I_{pa}) vs. scan rate (v) and (c) log I_{pa} vs. log v (scan rate).

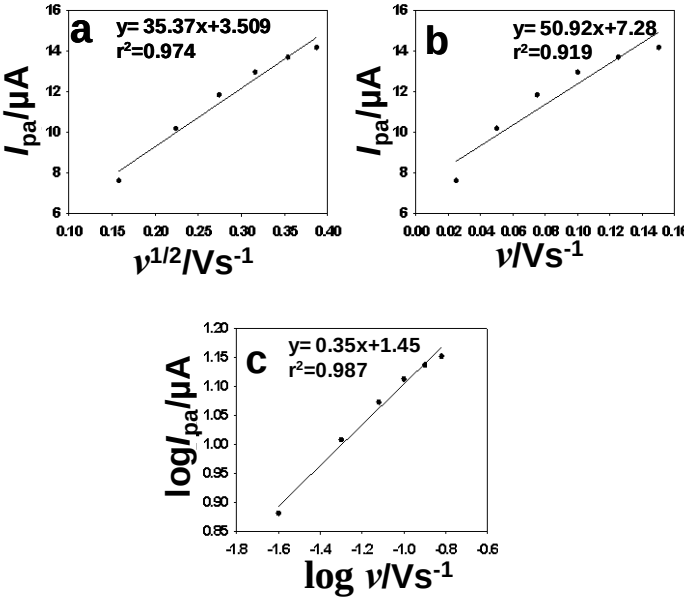

Figure 5. Various graphs obtained from the oxidation of 0.01 M Fc in [(C_2sulf) (NTf_2)] with Pt electrode: (a) Peak current (I_{pa}) vs. root square scan rate ($v^{1/2}$), (b) Peak current (I_{pa}) vs. scan rate (v) and (c) log I_{pa} vs. log v (scan rate).

oxidation peak in all three RTILs, the plot of logarithm of anodic peak current (log I_{pa}) vs. logarithm of scan rate (log v) was plotted. Fig 3c shows a plot of logarithm of peak current (log I_{pa}) vs. logarithm of scan rate (log v) for Fc oxidation in [(C_4mpyrr) (NTf_2)] in addition, Figure 4c and Figure 5c show the same plot for Fc oxidation in [(C_2mim) (OTf)] and [(C_2sulf) (NTf_2)], respectively. With the help of the above plots the slope value was calculated in order to find out the exact nature of Fc oxidation with Pt electrode in all three RTILs. The value of slopes were found to be a 0.84, 0.61

and 0.35 in [(C_4mpyrr) (NTf_2)], [(C_2mim) (OTf)] and [(C_2sulf) (NTf_2)], respectively. From these slope values, it is inferred that the oxidation of Fc with Pt electrode [(C_4mpyrr) (NTf_2)] and [(C_2mim) (OTf)] is mixed diffusion-adsorption controlled electrode process, since the slope value is greater than 0.5 [3, 26-27], however, in [(C_2sulf) (NTf_2)] a diffusion controlled electrode process is observed because the value of slope is less than 0.5.[26] The different slopes value indicates the nature of Fc oxidation in RTILs with Pt electrode are different, which may be attributed to the number of factors such as solubility of Fc, size of cation and anion and viscosities of RTILs etc.[28]

It is observed from the Table 1 that the type of RTIL affects the redox process of Fc with the Pt electrode. The $E_{1/2}$ of the Fc in different RTIL are tabulated in Table 1 considering that the diffusion coefficient for the Fc and Fc^+ are same[29] by using the following equation:

$$E_{1/2} = E_{pa} - \Delta E_p/2 \quad (1)$$

where, $E_{1/2}$ is half have potential (V), ΔE_p is the potential difference between anodic and cathodic peak. It has been observed that $E_{1/2}$ value is independent of scan rate in respective RTIL reflects the typical reversible behavior of redox couple.

Table 1. CV data for the redox process of Fc in different RTILs with Pt electrode at 25°C.

RTIL	v(mVs^{-1})	ΔE_p (V)	$E_{1/2}$/V	[I_{pa}/I_{pc}]
[(C_4mpyrr) (NTf_2)]	25	0.074	0.176	1.30
	50	0.077	0.177	1.32
	75	0.079	0.178	1.32
	100	0.079	0.178	1.33
	125	0.081	0.179	1.34
	150	0.081	0.179	1.37
[(C_2mim) (OTf)]	25	0.063	0.047	1.04
	50	0.063	0.045	1.02
	75	0.065	0.046	1.03
	100	0.070	0.046	1.04
	125	0.065	0.046	1.03
	150	0.068	0.047	1.03
[(C_2sulf) (NTf_2)]	25	0.078	0.227	1.01
	50	0.086	0.226	1.03
	75	0.098	0.230	1.05
	100	0.102	0.230	1.07
	125	0.108	0.232	1.09
	150	0.123	0.231	1.13

At each scan rate (v), I_{pa}/I_{pc} value for Fc lies in between 1.00 and 1.30 in all RTILs as summarized in Table 1, which is also one of the key criteria to judge the electrochemical reversibility of the system.[30-31] In case of [(C_4mpyrr) (NTf_2)], [(C_2mim) (OTf)] and [(C_2sulf) (NTf_2)] the I_{pa}/I_{pc} of Fc is approximately equal to unity shows the one electron reversible redox couple as reported elsewhere. [32-33] At each scan rate (v), the E_{pa} and E_{pc} for the Fc/Fc^+ redox system were independent of v, and I_{pa} increased with root scan rate ($v^{½}$) variation in all the three RTILs studied for Fc system. These observations are consistent with those expected for a freely diffusing species in a solution.[27]

The redox peak of Fc increases linearly with the increase in scan rate in accordance with Randles–Sevcik equation. The diffusion coefficient of Fc in all RTILs with Pt electrode are estimated according to the gradient of a linear plot of I_{pa} vs. $v^{½}$ plot, based on the Randles–Sevcik equation [34] is given by

$$I_{pa} = (2.69\times10^5)\, n^{3/2} A c D^{½} v^{1/2} \quad (2)$$

where, n is the number of electrons in charge transfer step, A is the electrode area (in cm^2), c is the concentration of electroactive species (in mol cm^{-3}), D is the diffusion coefficient (in $cm^2\ s^{-1}$) and v the potential sweep rate (in V s^{-1}). The calculated values of diffusion coefficient with the Pt electrode in the RTILs studied are compiled in Table 3. The diffusion coefficient with the Pt electrode in RTILs decreases in the order of [(C_2sulf) (NTf_2)] > [(C_2mim) (OTf)] > [(C_4mpyrr) (NTf_2)] (Table 3) which is similar to the decreasing trend of the viscosity of the RTILs as reported earlier.[23,35-37]

3.3 Electrochemical behavior of Fc in different RTIL with Au electrode

CVs for the oxidation of Fc in all the three RTILs with Au electrode at different scan rates from 25 to 150 mV s^{-1} is shown in Figure 6. Fc is oxidized to Fc^+ at the peak potential of (A) +0.157 V in [(C_4mpyrr) (NTf_2)], (B) +0.085 V in [(C_2mim) (OTf)] and (C) +0.257 V in [(C_2sulf) (NTf_2)] vs. Pt (at 50 mV s^{-1}) and reduced back to Fc at the potential of 0.081 V, 0.017 V and 0.181 V in [(C_4mpyrr) (NTf_2)], [(C_2mim) (OTf)] and [(C_2sulf) (NTf_2)], respectively (at 50 mV s^{-1}), showing one electron involvement for the redox system Fc/ Fc^+. For the oxidation of Fc to Fc^+ with Au electrode, the same mechanism can be given as described in section 3.1 for Pt electrode.

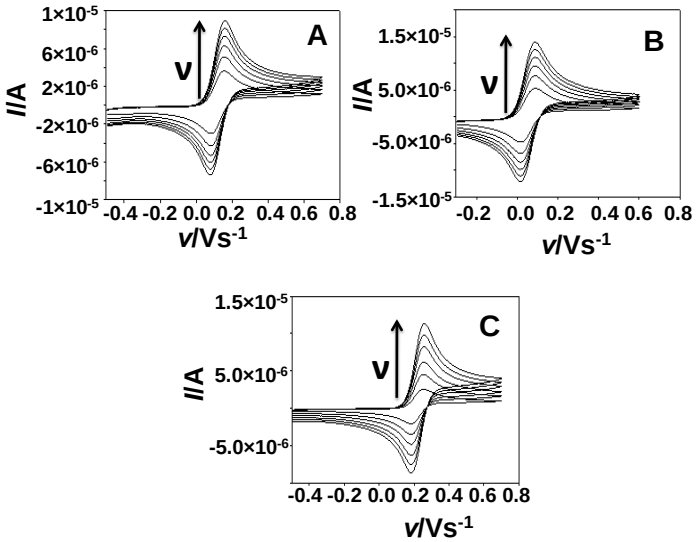

Figure 6. CVs for the oxidation of 0.01M Fc with Au electrode in the RTILs: (A) [(C_4mpyrr) (NTf_2)], (B) [(C_2mim) (OTf)] and (C) [(C_2sulf) (NTf_2)] at scan rates of 25, 50, 75, 100, 125 and 150 mV/s.

3.4. Effect of scan rate on Ferrocene at Au electrode

Scan rate variation studies were conducted by increasing the scan rate from 25 mV/s to150 mV/s with an increment of 25 mV/s in order to investigate the redox behavior of Fc with Au electrode. The Fc showed an increase in the peak current in all the three RTILs. The graph of I_{pa} vs. $v^{½}$ were plotted for Fc oxidation in all three RTILs and shown in Figs. 7, 8 and 9. Figure 7a shows a plot of I_{pa} vs. $v^{½}$ for Fc in [(C_4mpyrr) (NTf_2)], in addition, Figure 8a, and Figure 9a show the same plot for Fc in [(C_2mim) (OTf)] and [(C_2sulf) (NTf_2)], respectively. In all cases a high degree of linearity with anodic peak is observed for Fc with Au electrode (least square correlation coefficient 0.999 in [(C_4mpyrr) (NTf_2)] 0.999 in [(C_2mim) (OTf)] and 0.992 in [(C_2sulf) (NTf_2)]. Moreover, the I_{pa} vs. v variation profiles were also plotted (Figure 7b, 8b and 9b) and it shows good linearity (less than the $v^{½}$) and the least square correlation coefficient values are also approaching to 1.0).

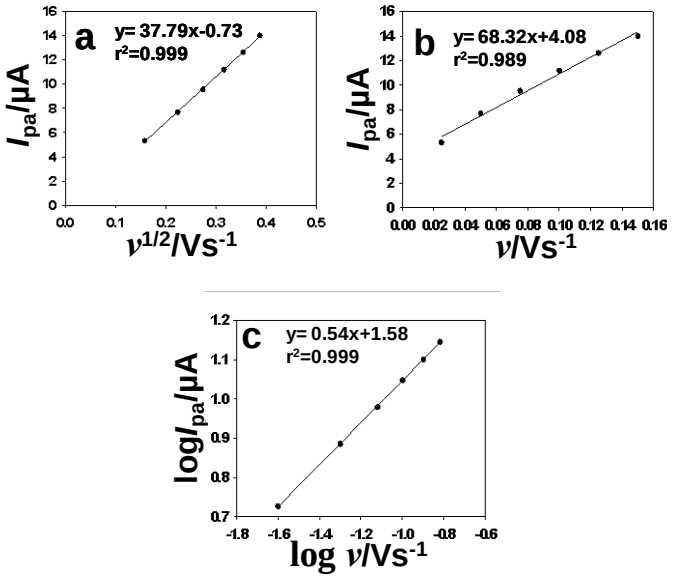

Figure 7. Various graphs obtained from the oxidation of 0.01 M Fc in [(C_4mpyrr) (NTf_2)] with Au electrode: (a) Peak current (I_{pa}) vs. root square scan rate ($v^{1/2}$), (b) Peak current (I_{pa}) vs. scan rate (v) and (c) log I_{pa} vs. log v (scan rate).

Therefore, to further confirm the behavior of Fc oxidation peak in all three RTILs, the plot of logarithm of peak current (log I_{pa}) vs. logarithm of scan rate (log v) was plotted.

Figure 7c shows a plot of logarithm of peak current (log I_{pa}) vs. logarithm of scan rate (log v) for Fc in [(C_4mpyrr) (NTf_2)] in addition, Figure 8c, and Figure 9c show the same plot for Fc in [(C_2mim) (OTf)] and [(C_2sulf) (NTf_2)], respectively. The values of slope were found to be a 0.50, 0.54 and 0.83 in [(C_4mpyrr) (NTf_2)], [(C_2mim) (OTf)] and [(C_2sulf) (NTf_2)], respectively. From these slope values it can be inferred that the oxidation of Fc with Au electrode in [(C_4mpyrr) (NTf_2)] and [(C_2mim) (OTf)] is diffusion controlled electrode process, since the slope value is close to the theoretical value of 0.5 that is expressed for an ideal reaction for diffusion controlled electrode process and in [(C_2sulf) (NTf_2)] it shows an mixed diffusion-adsorption controlled process,

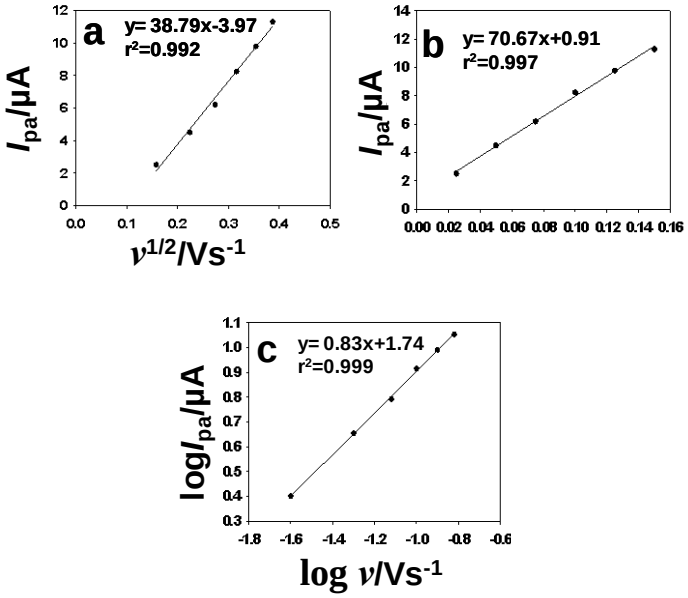

Figure 8. Various graphs obtained from the oxidation of 0.01 M Fc in [(C_2mim) (OTf)] with Au electrode: (a) Peak current (I_{pa}) vs. root square scan rate ($v^{½}$) (b) Peak current (I_{pa}) vs. scan rate (v) and (c) log I_{pa} vs. log v (scan rate).

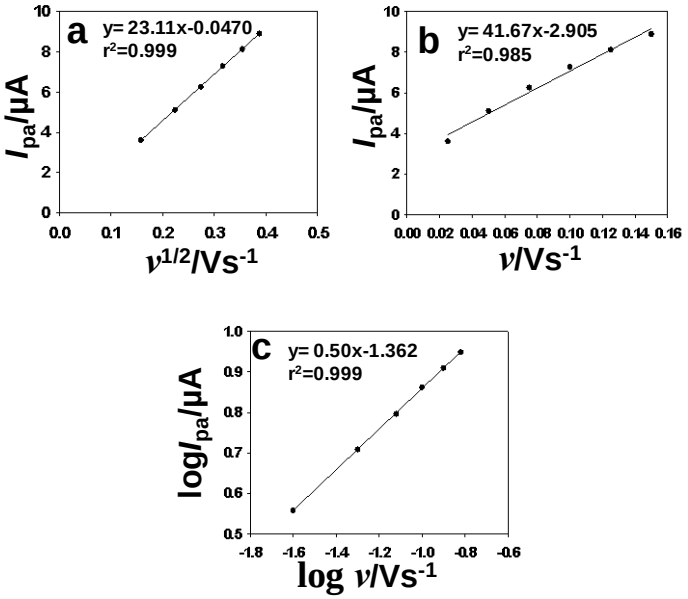

Figure 9. Various graphs obtained from the oxidation of 0.01 M Fc in [(C_2sulf) (NTf_2)] with Au electrode: (a) Peak current (I_{pa}) vs. root square scan rate ($v^{½}$), (b) Peak current (I_{pa}) vs. scan rate (v) and (c) log I_{pa} vs. log v (scan rate).

since the slope value is greater than 0.5 adsorption. Therefore, with the help of these data it is concluded that the nature of Fc oxidation in RTILs is not only based on the types of RTIL used, however, it also depends on the nature of working electrode material as reported earlier for glassy carbon, Au and Pt electrode. [38]

Table 2 summarizes the calculated values of ΔE_p, $E_{1/2}$ and I_{pa}/I_{pc} for the oxidation of 0.01 M of Fc with Au electrode in all the three RTILs. It is observed from Table 2 that, at each scan rate, the I_{pa}/I_{pc}

approximately equal to unity in all the RTILs studied, indicating reversible behavior of Fc redox couple with Au electrode while in case of Pt electrode in [(C_2sulf) (NTf_2)], Fc shows quasi reversible behavior. Moreover, it is found that the peak potential values were independent of scan rate showing reversible behavior of Fc in all RTILs.

The $E_{1/2}$ of the couple in all RTILs was calculated and it is found that the value of $E_{1/2}$ is not varying with scan rate variation or it is independent of scan rate as required by reversible couple. Interestingly, as can be seen from Table 1 and Table 2, both in case of Pt and Au, $E_{1/2}$ value is same, which shows that $E_{1/2}$ is independent of electrode material. From Table 1 and 2 it can also be inferred that, $E_{1/2}$ value is dependent on the composition and physical properties of electrolyte as in different RTIL values of $E_{1/2}$ changes.

Table 2. CV data for the redox process of Fc with Au electrode in different RTILs at 25ºC.

Elec	RTIL	Diffusion coefficient *(D)* cm^2/s	η (cP)	$D\eta$ (cm g s^{-2})	Ref.
Pt	[(C_4mpyrr) (NTf_2)]	0.404×10^{-7}	89 [43]	0.36×10^{-7}	This work
	[(C_2mim) (OTf)]	1.16×10^{-7}	45 [43]	0.52×10^{-7}	This work
	[(C_2sulf) (NTf_2)]	1.75×10^{-7}	30 [43]	0.53×10^{-7}	This work
Au	[(C_4mpyrr) (NTf_2)]	0.70×10^{-7}	89	0.62×10^{-7}	This work
	[(C_2mim) (OTf)]	2.0×10^{-7}	45	0.90×10^{-7}	This work
	[(C_2sulf) (NTf_2)]	2.10×10^{-7}	30	0.63×10^{-7}	This work
	Molecular liquid				
	ACN	224×10^{-7}	0.34	0.8×10^{-7}	44
	DMSO	44×10^{-7}	1.99	0.9×10^{-7}	44
	DCM	167×10^{-7}	0.41	0.7×10^{-7}	44
	DMF	95×10^{-7}	0.80	0.8×10^{-7}	44

This variation of $E_{1/2}$ in different RTILs is due to difference in physical properties of RTILs such as dielectric constant, viscosity, dipole moment etc. Moreover, it is also observed that the ΔE_p values obtained at slow scan rate are consistent in both Pt and Au electrode and at higher scan rate greater than 100 mV s^{-1}, values of ΔE_p increase as expected when a low level of uncompensated resistance is present.[16] From all these observations it is inferred that Pt wire can used as quasi-reference electrode since the oxidation of Fc with Pt and Au electrode shows same quasi-reversible behavior with Fc.

The diffusion coefficient of 0.01 M Fc in all RTILs with Au electrode was estimated according to the gradient of a linear plot of I_{pa} vs. $v^{½}$ plot, based on the Randles-Sevcik equation. The calculated value of diffusion coefficient of Fc in all three RTILs with Au electrode is summarized in Table 3. The calculated values of diffusion coefficient with Au electrode in all three RTILs are in the order of [(C_2sulf) (NTf_2)] > [(C_2mim) (OTf)] > [(C_4mpyrr) (NTf_2)]. The highest diffusion coefficient obtained for [(C_2sulf) (NTf_2)] is in agreement with its lower viscosity when compared to other RTILs. In general, diffusion coefficients of ferrocene are on the order of 10^{-7} cm^2 s^{-1} which is two orders of magnitude lower than in conventional solvents.[39-40] These results suggest that, if the RTILs viscosity is less, then the diffusion of Fc will be more, which in turn reflects higher value of diffusion coefficient.

A graph is plotted between diffusion coefficient and reciprocal of viscosity as per the Stokes –Einstein equation [41] as given below:

$$D\eta = BT/6\pi r \quad (3)$$

Where, D is diffusion coefficient, η is viscosity, T is temperature, B is the Boltzmann constant and r is the Fc radius. Moreover, this equation is also used to observe the hydrodynamic radius of diffusing species. Based on D and η value (based on reported viscosity earlier [28] product of $D\eta$ are calculated and presented in Table 3.

Table 3. Diffusion coefficients of Fc in different RTILs with Pt and Au electrodes.

RTIL	v (mVs^{-1})	ΔEp (V)	$E_{1/2}$ (V)	[i_{pa}/i_{pc}]
[(C_4mpyrr) (NTf_2)]	25	0.075	0.189	0.998
	50	0.085	0.189	1.013
	75	0.09	0.192	1.026
	100	0.096	0.192	1.039
	125	0.01	0.192	1.051
	150	0.102	0.193	1.062
[(C_2mim) (OTf)]	25	0.066	0.053	1.07
	50	0.066	0.055	1.06
	75	0.066	0.055	1.06
	100	0.066	0.053	1.06
	125	0.066	0.053	1.06
	150	0.068	0.054	1.06
[(C_2sulf) (NTf_2)]	25	0.073	0.223	0.955
	50	0.078	0.224	0.962
	75	0.071	0.223	0.967
	100	0.071	0.223	0.973
	12 5	0.071	0.224	0.974
	150	0.071	0.224	0.974

As can be seen from the Table 3, that $D\eta$ value is in the range of $0.6\pm0.3\times10^{-7}$ cm g S^{-2}. From the above results it can be concluded that Fc radius is constant in RTIL and organic solvents and independent of the medium. [23, 42] $D\eta$ value of Fc in molecular liquid is in the range of $0.8\pm0.1\times10^{-7}$ cm g S^{-2}.[44] A graph is plotted between D and 1/ η for three ionic liquid viz. [(C_2sulf) (NTf_2)], [(C_2mim) (OTf)] and [(C_4mpyrr) (NTf_2)] at Pt (Fig 10A) and Au (Fig 10B) electrode and it has been observed that both the curve exhibits linearity and passes through origin. [41] The Fc radius

calculated from the slope of the line and above equation, the radius of Fc is 0.57 nm was determined which is slightly larger than crystallographic radius of Fc due to interaction of Fc and anionic species of RTIL as reported elsewhere.[41]

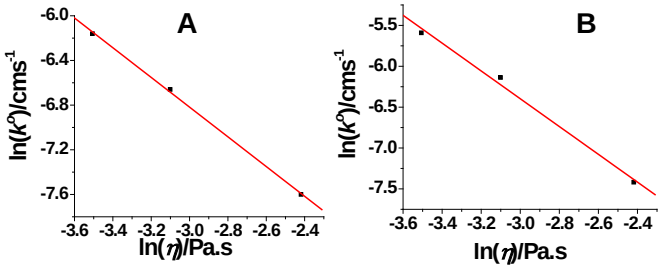

Figure 10. Stokes-Einstein plot of diffusion coefficient (D) vs. 1/viscosity (η^{-1}) for ferrocene at (A) Pt and (B) Au electrode with three different RTILs.

In order to understand the thermodynamic process involved in Fc oxidation process in RTIL a graph is plotted between ln (k^o) versun ln (η) as per the following equation:

$$\ln(k^o)=[\ln(A)-\Delta G/RT]-\theta\ln(3V\mathrm{m}\xi\alpha/\xi_0 RT)-\theta\ln(\eta) \quad (4)$$

where, A is the portion of pre exponential factor, θ is a fraction that depends on the degree of reaction adiabatically, Vm molar volume of medium and $\xi\alpha$ and ξ_0 are the high frequency and static permittivity, respectively. Rest of symbols is its standard abbreviation. As can be seen from the Fig 11 A and B ln (k^o) versus ln (η) shows linear relationship with linear regression >0.99. With slope value of Fig 11A and B shows that Fc process in RTIL with Pt and Au electrodes are adiabatic and linear relationship between ln (k^o) versus ln (η) depicts that the RTIL structure has negligible effect on the k^o value as reported earlier. [41]

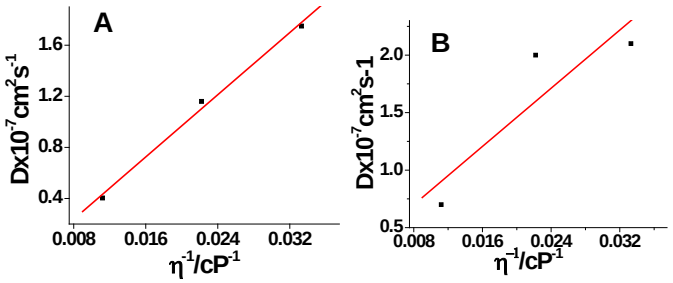

Figure 11. Plot of ln (k^o) versus ln (η) for ferrocene at (A) Pt and (B) Au electrode with three different RTILs.

3.5. Electrochemical impedance spectroscopic characterization of Fc at Pt and Au electrode

In this study, EIS was employed to get information on the impedance changes of the electrode surface during the redox process of Fc in all three RTILs. The diameter of the semicircle usually equals to the electron transfer resistance, which controls the electron transfer kinetics of the redox probe at the electrode interface.[43,44] Charge transfer resistance (R_{ct}) was estimated using Nyquist plot of high frequency semicircle region.

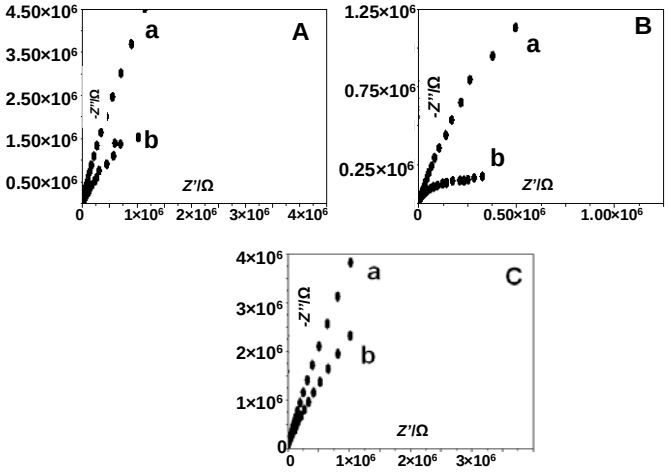

Figure 12. Nyquist plot of Fc with Pt electrode at OCP (A) in [(C_4mpyrr) (NTf_2)] (a) RTIL without Fc and (b) with 0.01 M Fc, (B) in [(C_2mim) (OTf)] (a) RTIL without Fc and (b) with 0.01 M Fc and (C) in [(C_2sulf) (NTf_2)] (a) RTIL without Fc and (b) with 0.01 M Fc.

Randles equivalent circuit was used to estimate the value of R_{ct} and the electrical double layer capacitance (C_{dl}) and the data validation carried out by the Kramers-Kronig (KK) test from the FRA software of Metrohm autolab, prove that experimental results fit reasonably and are in a good agreement with the proposed circuit model.

Figures 12Aa, 12Ba and 12Ca illustrate the typical results of AC impedance spectra of the neat RTILs with Pt electrode in [(C_4mpyrr) (NTf_2)], [(C_2mim) (OTf)] and [(C_2sulf) (NTf_2)], respectively. Figs. 12Ab, 12Bb, and 12Cb represent the impedance spectra after the addition of 0.01 M Fc in [(C_4mpyrr) (NTf_2)], [(C_2mim) (OTf)] and [(C_2sulf) (NTf_2)], respectively.

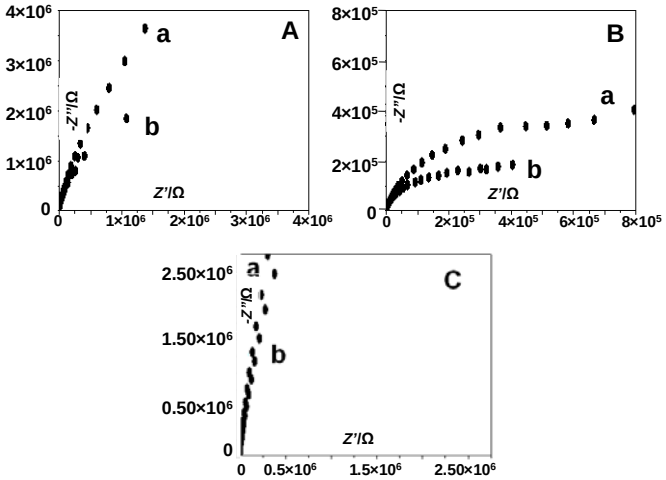

Figure 13. Nyquist plot of Fc with Au electrode at OCP (A) in [(C_4mpyrr) (NTf_2)] (a) RTIL without Fc and (b) with 0.01 M Fc, (B) in [(C_2mim) (OTf)] (a) RTIL without Fc and (b) with 0.01 M Fc and (C) in [(C_2sulf) (NTf_2)] (a) RTIL without Fc and (b) with 0.01 M Fc.

Figures 13Aa, 13Ba and 13Ca show the AC impedance spectra of the neat RTILs with Au electrode in [(C_4mpyrr) (NTf_2)],

[(C_2mim) (OTf)] and [(C_2sulf) (NTf_2)], respectively. Figs. 13Ab, 13Bb and 13Cb represents the impedance spectra after the addition of 0.01 M Fc in [(C_4mpyrr) (NTf_2)], [(C_2mim) (OTf)] and [(C_2sulf) (NTf_2)], respectively. In Fig 12 and 13, the semicircle is partially resolved at higher frequency corresponds to the R_{ct} while at lower frequency the straight line of Nyquist plot inclined at -45 degree with Z' axis. EIS results conferred that at Pt and Au electrode the diffusion of Fc is the slowest step and hence rate determining step.[29] All the obtained results reveal that after the addition of 0.01 M Fc, R_{ct} value is decreased for all RTILs irrespective of nature of electrode used. This attributes the acceleration of charge transfer due to the presence of Fc in RTILs.

The values of R_{ct} and C_{dl} with the Pt and Au electrodes in all the RTILs studied are compiled and presented in Table 4. It is important to mention that all the calculated values of R_{ct} and C_{dl} reported here are at open circuit potential (OCP). From Table 4, it is evident that, the RTIL having high viscosity, the value of R_{ct} is more as diffusion of Fc molecule is slow when compared with low viscosity RTIL. The capacitance values are compared after the addition of Fc for the all three RTILs studied with Pt and Au electrode, the following relation is observed: [(C_2sulf) (NTf_2)]> [(C_2mim) (OTf)] > [C_4mpyrr] [NTf_2], which is similar to the decreasing trend of the viscosity of RTILs. These results suggest that capacitance decreases with increasing the viscosity of RTILs. It is noteworthy to mention an increase in C_{dl} is observed after the addition of Fc in RTILs as indicated in Table 4 same trend is reported earlier.[45,46]

Table 4. Values of the equivalent circuit parameters of the fitting curves for without and ferrocene with Pt and Au electrode

Elec	RTIL	Fc/M	R_{ct}/kΩ	C_{dl} ×10^{-6}	n
Pt	[(C_4mpyrr) (NTf_2)]	0	0.650	0.652	0.907
		0.01	0.635	0.675	0.899
	[(C_2mim) (OTf)]	0	0.253	0.370	0.854
		0.01	0.176	0.389	0.832
	[(C_2sulf) (NTf_2)]	0	0.213	0.308	0.923
		0.01	0.102	0.698	0.920
Au	[(C_4mpyrr) (NTf_2)]	0	0.809	0.841	0.946
		0.01	0.627	0.961	0.936
	[(C_2mim) (OTf)]	0	0.335	0.833	0.910
		0.01	0.296	0.901	0.914
	[(C_2sulf) (NTf_2)]	0	0.212	0.378	0.964
		0.01	0.180	0.426	0.958

The apparent heterogeneous rate constant (k^o), for the Fc/Fc^+ was studied by electrochemical impedance spectroscopy in [(C_4mpyrr) (NTf_2)], [(C_2mim) (OTf)] and [(C_2sulf) (NTf_2)], containing 0.01 M Fc/Fc^+ using Nyquist plot shown in Figure 12 and 13 on a Pt and Au electrode, respectively.

The Randless equivalent circuit model was used for the calculation of R_{ct}. k^o is represented by following equation:[47]

$$R_{ct}=RT/FI_0 \quad (5)$$

$$I_0 = FAk^{\circ}c_o^{*(1-\alpha)}c_R^{*\alpha} \quad (6)$$

where, I_0 is the exchange current, A is the area of electrode, c_o * and c_R * are the bulk concentration of the oxidized and the reduced form, is the transfer coefficient, R is the gas constant, and T is the absolute temperature.

Table 5: The apparent heterogeneous rate constant (k^o) of Fc redox couples in different ionic liquid at 25°C using Pt and Au electrode

Electrode	RTIL	k^o (cm s^{-1})
Pt	[(C_4mpyrr) (NTf_2)]	0.06 ×10^{-2}
	[(C_2mim) (OTf)]	0.216 ×10^{-2}
	[(C_2sulf) (NTf_2)]	0.373 ×10^{-2}
Au	[(C_4mpyrr) (NTf_2)]	0.05 ×10^{-2}
	[(C_2mim) (OTf)]	0.128 ×10^{-2}
	[(C_2sulf) (NTf_2)]	0.211 ×10^{-2}

The k^o values for Fc in ionic liquids were estimated in different ionic liquids at Pt and Au electrodes and are summarized in Table 5. Analysis of data in Table 5, reveal that the k^o values are decreasing by virtue of viscosity of RTIL and showing inverse relationship with the viscosity at both the electrode. This finding can be explained by the Marcus expression for the k^o in conventional electrolyte by the following equation[48]:

$$k^o = k\theta Z_{het}\, e^{(-\Delta Gexp/RT)} \quad (7)$$

where, ΔG_{exp} is the apparent activation energy, k is the transfer coefficiemt, θ is the displacement fluctuation parameter, Z_{het} is the collision frequency factor (Z_{het}=4.57×10^3cm s^{-1} at T 294.15K), R is universal gas constant and T is absolute temperature. It has been observed that the Fc redox behavior at Pt and Au electrode governed by the outer sphere redox reaction as no chemical bond formation and breaking take place.[49,50] Being an adiabatic process as observed by a graph between ln (k^o) versus ln (η) and consequently the product of $k\theta$ are equal to unity, the ΔG_{exp} for Fc on both the electrode was calculated from the equation 7 and presented in table 5. Through the above results of table 5, it can be concluded that the k^o value is dependent on the viscosity of medium and will be lower in high viscous RTIL owing to lower analyte diffusion and ΔG_{exp} will be higher in the RTILs due to increased solvent reorganization energy, as reported earlier.[46] Therefore, the value of k^o decreases with increasing viscosity of RTIL as tabulated in Table 5. The above results reflects the rate of electron transfer of the Fc system at Pt and Au electrode is greatly affected by the thermodynamic parameters as they are very sensitive to viscosity of electrolyte used.

CONCLUSIONS

In the present work, electrochemical characterization of Fc with Pt and Au electrode in [(C_4mpyrr) (NTf_2)], [(C_2mim) (OTf)] and [(C_2sulf) (NTf_2)] were successfully investigated by utilizing CV and EIS technique. On both the Pt and Au electrode, almost similar half-wave potential is observed in respective ionic liquid indicating

that working electrode material had a negligible effect on $E_{1/2}$. Diffusion coefficient of Fc in all the three RTILs was obtained and it was found that the value of diffusion coefficient is inversely dependent on the viscosity of RTIL as per the Stokes-Einstein relation. The apparent heterogeneous rate constant (k^o) was determined by EIS data which is found of the order of 10^{-2} cm s^{-1} which are smaller than those in aqueous and organic solution. A variation in k^o with different RTIL shows there is inverse relationship with the viscosity of RTIL. A graph between ln (k^o) versus ln (η) suggests that Fc process in RTIL with Pt and Au electrodes are adiabatic. With help of CV it was found that the redox nature of Fc in the studied RTILs indicates that the process is shows reversible electrochemical reaction kinetics. EIS data confirms the diffusion of Fc in RTIL is the slowest and rate determining step. Apparent activation energy (ΔG_{exp}) was calculated and found that it depends on the viscosity of RTIL.

ACKNOWLEDGEMENT

The authors thank Dr. D. K. Dubey, Director, Defence Research and Development Establishment, DRDO, Gwalior-474002 (India) for his keen interest and encouragement. This manuscript is assigned DRDE accession no. DRDE/PD/12/2019.

REFERENCES

1. M. Gras, N. Papaiconomou, N. Schaeffer, E. Chainet, F. Tedjar, J. A. Coutinho, I. Billard. Ionic liquid based acidic aqueous biphasic systems for simultaneous leaching and extraction of metallic ions. *Angew. Chemie. Int. Ed.* **2018**, *57*, 1563-1566.
2. A.P. Abbott, R. C. Harris, F. Holyoak, G. Frisch, J. Hartley, G. R. Jenkin. Electrocatalytic recovery of elements from complex mixtures using deep eutectic solvents. *Green. Chem.* **2015**, *17*, 2172-2179.
3. N. Frenzel, J. Hartley, G. Frisch. Voltammetric and spectroscopic study of ferrocene and hexacyanoferrate and the suitability of their redox couples as internal standards in ionic liquids. *Phy. Chem. Chem. Phys.* **2017**, *19*, 28841-28852.
4. N. I. M. F. Hilmy, W. Z. N. Yahya, K. A. Kurnia, Eutectic ionic liquids as potential electrolytes in dye-sensitized solar cells: Physicochemical and conductivity studies, *J. Mol. Liq.* **2020**, *320*, 114381-114384.
5. B. Siwach, S. Sharma, D. Mohan. Structural, optical and morphological properties of ZnO/MWCNTs nanocomposite photoanodes for Dye Sensitized Solar Cells (DSSCs) application. *J. Integr. Sci. Technol.*, **2017**, *5*(1), 1-4.
6. P. Ma, Y. Fang, N. Fu, X. Zhou, S. Fang, Y. Lin. Ionic conductivity enhancement of "soggy sand" electrolytes with AlOOH nanofibers for dye-sensitized solar cells. *Electrochim. Acta* **2020**, *337*, 135849-135857.
7. H. Sun, G. Zhu, X. Xu, M. Liao, Y.-Y. Li, M. Angell, M. Gu, Y. Zhu, W. H. Hung, J. Li. A safe and non-flammable sodium metal battery based on an ionic liquid electrolyte. *Nat. commun.* **2019**, *10*, 1-11.
8. S. A. Goodchild, L. J. Hubble, R. K. Mishra, Z. Li, K. Y. Goud, A. Barfidokht, R. Shah, K. S. Bagot, A. J. McIntosh, J. Wang. Ionic liquid-modified disposable electrochemical sensor strip for analysis of fentanyl. *Anal. Chem.* **2019**, *91*, 3747-3753.
9. E. Guinea, A. Salicio-Paz, A. Iriarte, H. J. Grande, E. Medina, E. García-Lecina. Robust aluminum electrodeposition from ionic liquid electrolytes containing light aromatic naphta as additive. *Chemistry Open*, **2019**, *8*, 1094-1099.
10. M.V. Bhute, Y.P. Mahant, S.B. Kondawar. Titanium dioxide / poly(vinylidene fluoride) hybrid polymer composite nanofibers as potential separator for lithium ion battery. *J. Mater. Nanosci.* **2017**, 4 (1), 6–12.
11. D. Bengio, E. Mendes, S. Pellet-Rostaing, P. Moisy. Electrochemical behavior of platinum and gold electrodes in the aprotic ionic liquid N, N-Trimethylbutylammonium bis (trifluoromethanesulfonyl) imide. *J. Electroanal. Chem.* **2018**, *823*, 445-454.
12. M. Thakurathi, E. Gurung, M. M. Cetin, V. D. Thalangamaarachchige, M. F. Mayer, C. Korzeniewski, E. L. Quitevis. The Stokes-Einstein equation and the diffusion of ferrocene in imidazolium-based ionic liquids studied by cyclic voltammetry: Effects of cation ion symmetry and alkyl chain length. *Electrochim. Acta* **2018**, *259*, 245-252.
13. L. Nagy, G. Gyetvai, L. Kollár, G. Nagy. Electrochemical behavior of ferrocene in ionic liquid media. *J. Biochem. Biophys. Methods* **2006**, *69*, 121-132.
14. Y. Matsubara. Solvent Effect on Ferrocenium/Ferrocene Redox Couple as an Internal Standard in Acetonitrile and a Room-temperature Ionic Liquid. *Chem. Lett.* **2020**, *49*, 54-56.
15. Y. Pan, W. E. Cleland Jr, C. L. Hussey. Heterogeneous electron transfer kinetics and diffusion of ferrocene/ferrocenium in bis (trifluoromethylsulfonyl) imide-based ionic liquids. *J. Electrochem. Soc.* **2012**, *159*, F125-F133.
16. S. Eisele, M. Schwarz, B. Speiser, C. Tittel. Diffusion coefficient of ferrocene in 1-butyl-3-methylimidazolium tetrafluoroborate–concentration dependence and solvent purity. *Electrochim. acta* **2006**, *51*, 5304-5306.
17. P. Ugo, L. M. Moretto, M. De Leo, A. P. Doherty, C. Vallese, S. Pentlavalli. Diffusion regimes at nanoelectrode ensembles in different ionic liquids. *Electrochim. acta* **2010**, *55*, 2865-2872.
18. A.R. Neale, C. Schütter, P. Wilde, P. Goodrich, C. Hardacre, S. Passerini, A. Balducci, J. Jacquemin. Physical–chemical characterization of binary mixtures of 1-Butyl-1-methylpyrrolidinium bis {(trifluoromethyl) sulfonyl} imide and aliphatic nitrile solvents as potential electrolytes for electrochemical energy storage applications. *J. Chem. Eng. Data* **2017**, *62*, 376-390.
19. P.D. Virutkar, A.P. Mahajan, B.H. Meshram, S.B. Kondawar. Conductive polymer nanocomposite enzyme immobilized biosensor for pesticide detection. *J. Mater. Nanosci.* **2019**, 6 (1), 7–12.
20. K. Prasadini, K. Perera, K. Vidanapathirana. -Ethyl-3-methylimidazolium trifluoromethanesulfonate-based gel polymer electrolyte for application in electrochemical double-layer capacitors. *Ionics* **2019**, *25*, 2805-2811.
21. A. Deferm, J. C. Malaquias, B. Onghena, D. Banerjee, J. Luyten, H. Oosterhof, J. Fransaer, K. Binnemans. Electrodeposition of indium from the ionic liquid trihexyl (tetradecyl)phosphonium chloride. *Green. Chem.* **2019**, *21*, 1517-1530.
22. E. I. Rogers, D. S. Silvester, D. L. Poole, L. Aldous, C. Hardacre, R. G. Compton. Voltammetric characterization of the ferrocene|ferrocenium and cobaltocenium| cobaltocene redox couples in RTILs. *J. Phys. Chem. C* **2008**, *112*, 2729-2735.
23. A.K. Gosser, *Cyclic voltammetry: simulation and analysis of reaction mechanisms*, *Vol. 43*, VCH New York, **1993**.
24. A. Lewandowski, L. Waligora, M. Galinski. Ferrocene as a reference redox couple for aprotic ionic liquids. *Electroanalysis* **2009**, *21*, 2221-2227.
25. A.S. Silvester, K. R. Ward, L. Aldous, C. Hardacre, R. G. Compton. The electrochemical oxidation of hydrogen at activated platinum electrodes in room temperature ionic liquids as solvents. *J. Electroanal. Chem.* **2008**, *618*, 53-60.
26. A.J. Bard, L. R. Faulkner, J. Leddy, C. G. Zoski, *Electrochemical methods: fundamentals and applications. New York: Wiley* **1980**, *290*.
27. A.J. Bard, L. R. Faulkner, *Electrochemical Methods* **2001**, *2*, 580.
28. H. Ohno, *Electrochemical aspects of ionic liquids*, John Wiley & Sons, **2005**.
29. N. G. Tsierkezos, U. Ritter. Electrochemical impedance spectroscopy and cyclic voltammertry of ferrocene in acetonitrile/acetone system. *J. Appl. Electrochem.* **2010**, *40*, 409-417.
30. R. S. Nicholson, I. Shain. Theory of stationary electrode polarography. Single scan and cyclic methods applied to reversible, irreversible and kinetic systems. *Anal. Chem.* **1964**, *36*, 706-723.
31. A.R. Schrage, Z. Zhao, A. Boika, C. J. Ziegler. Evaluating ferrocene ions and all-ferrocene salts for electrochemical applications. *J. Organomet. Chem.* **2019**, *897*, 23-31.
32. J. Zhang, A. M. Bond. Conditions required to achieve the apparent equivalence of adhered solid-and solution-phase voltammetry for ferrocene and other redox-active solids in ionic liquids. *Anal. Chem.* **2003**, *75*, 2694-2702.

33. A. Barrado, R. Couto, M. Quinaz, J. Lima, Y. Castrillejo. Electrochemical behaviour of ferrocene in the ionic liquid 1-ethyl-3-methylimidazolium tetrafluoroborate, EMIMBF4, at 298 K. *J. Electroanal. Chem.* **2014**, *720*, 139-146.
34. Wang, J.: Analytical Electrochemistry, 2nd Ed. John Wiley & Sons, New York **2005**.
35. S. Jiang, Y. Hu, Y. Wang, X. Wang. Viscosity of Typical Room-Temperature Ionic Liquids: A Critical Review. *J. Phys. Chem.* **2019**, *48*, 033101.
36. P. Barthen, W. Frank, N. Ignatiev. Development of low viscous ionic liquids: the dependence of the viscosity on the mass of the ions. *Ionics* **2015**, *21*, 149-159.
37. A.Y. Kim, J.C. Yang, H.W. Kim, G.M. Swain. Heterogeneous electron-transfer rate constants for ferrocene and ferrocene carboxylic acid at boron-doped diamond electrodes in a room temperature ionic liquid. *Electrochim. Acta*, **2013**, *94*, 49-56.
38. V.M. Hultgren, A. W. Mariotti, A.M. Bond, A.G. Wedd. Reference potential calibration and voltammetry at macrodisk electrodes of metallocene derivatives in the ionic liquid [bmim][PF6]. *Anal. Chem.* **2002**, *74*, 3151-3156.
39. P. Hapiot, C. Lagrost. Electrochemical reactivity in room-temperature ionic liquids. *Chem. Rev.* **2008**, *108*, 2238-2264.
40. N.G. Tsierkezos. Cyclic Voltammetric Studies of Ferrocene in Nonaqueous Solvents in the Temperature Range from 248.15 to 298.15 K. *J. Solution. Chem.* **2007**, *36*, 289-302.
41. A.L. Bentley, J. Li, A. M. Bond, J. Zhang. Mass-transport and heterogeneous electron-transfer kinetics associated with the ferrocene/ferrocenium process in ionic liquids. *J. Phy. Chem.* C **2016**, *120*, 16516-16525.
42. A. Lewandowski, L. Waligora, M. Galinski. Electrochemical behavior of Cobaltacene in Ionic liquids. *J. Solution. Chem.* **2013**, *42*, 251-262.
43. J. Morales-Ugarte, A. Benayad, C. Santini, R. Bouchet. Electrochemical Impedance Spectroscopy and X-ray Photoelectron Spectroscopy Study of Lithium Metal Surface Aging in Imidazolium-Based Ionic Liquid Electrolytes Performed at Open-Circuit Voltage. *ACS Appl. Mater. Interfaces* **2019**, *11*, 21955-21964.
44. R. Fortunato, L. C. Branco, C. A. Afonso, J. Benavente, J. G. Crespo. Electrical impedance spectroscopy characterisation of supported ionic liquid membranes. *J. Membr. Sci.* **2006**, *270*, 42-49.
45. M.J. Shiddiky, A.A. Torriero, J.M. Reyna-González, A.M. Bond. Nonadditivity of Faradiac currents and modification of double layer capacitance in the voltammetry of mixture of ferrocene and ferrocenium salts in ionic liquid. *Anal. Chem.***2010**, *82*, 1680-1691.
46. N. Tachikawa, Y. Katayama, T. Miura. Electrode kinetics of some Iron complexes in an Imide –Type Room Temperature Ionic liquid. *ECS Transactions* **2007**, *3*, 577-589.
47. N. Tachikawa, Y. Katayama, T. Miura, Electrode kinetics of Ferocenium/Ferrocene in room temperature ionic liquids. *ECS Transactions* **2009**, *16*, 589-595.
48. J. Wallauer, K. Jähme, A. Venker, P. Kübler, J. Sundermeyer, B. Roling. Electrochemical kinetics of ferrocene based redox ILs investigated by multi spectrum impedance fitting. *J. Phys. Chem. C* **2017**, *121*, 26706-26712.
49. D. Uthra, R. Singh. Fascinating current density features of noble metal doped YBa2Cu3O7-δ (YBCO) Superconducting materials. *J. Integr. Sci. Technol.* **2019**, *7*(1), 10-13.
50. J.A. Riddick, W. B. Bunger, T. K. Sakano, Organic Solvents, Physical properties and methods of purification, 3rd ed., Wiley, Interscience, New York **1986**.